

Quarterly Progress Report

This report covers the period of December 15, 2015 to March 14, 2016

Submitted to

The Office of Naval Research

Project Title: Noise of High-Performance Aircraft at Afterburner

Principal Investigator

Dr. Christopher Tam

Department of Mathematics

Florida State University

Email: tam@math.fsu.edu

Grant Monitor

Dr. John Spyropoulos

Email: John.Spyropoulos@jsf.mil

During this quarter, our research effort concentrated on processing and understanding the real time noise data of the F-18E aircraft. There are two distinct parts to such an effort. The research to be reported here is confined to the traditional analysis. The primary goal is to obtain narrow band spectra. With narrow band spectra computed, we will be able to make direct comparisons with 1/3 octave band spectra (converted to narrow band) for the purpose of confirming data accuracy. It is also a priority of ours to examine narrow band data spectra carefully for details that are beyond the resolution of 1/3 octave band spectrum, such as unexpected peaks. Beyond standard jet noise data analysis, namely focusing primarily on noise intensity, spectrum and directivity, one can go further. In the literature, so far no one appears to have carried out an examination of the transient behavior of jet noise. The widely known phenomenon of “crackle” is, perhaps, a manifestation of transient behavior. Transient analysis of jet noise is not well established. Although it is not a task in the original proposal of this project yet we hope to be able to perform a preliminary study before the end of this project.

1. Computation of narrow band spectra

There are two well-established methods for computing narrow band spectrum from real time noise data. We shall refer to them as the Direct Computation Method and the Two-step Method.

In the Direct Computation Method, one starts with a fairly long data sample of length $2T_0$. Let the data sample be $p(t)$, $-T_0 \leq t \leq T_0$. The following computations are to be performed to obtain the noise spectrum $S(\omega)$.

$$p(\omega) \Big|_{T_0 \rightarrow \infty} = \frac{1}{2\pi} \int_{-T_0}^{T_0} p(t) e^{i\omega t} dt \quad (1)$$

$$S(\omega) \Big|_{T_0 \rightarrow \infty} = \frac{2\pi |p(\omega)|^2}{2T_0} \quad (2)$$

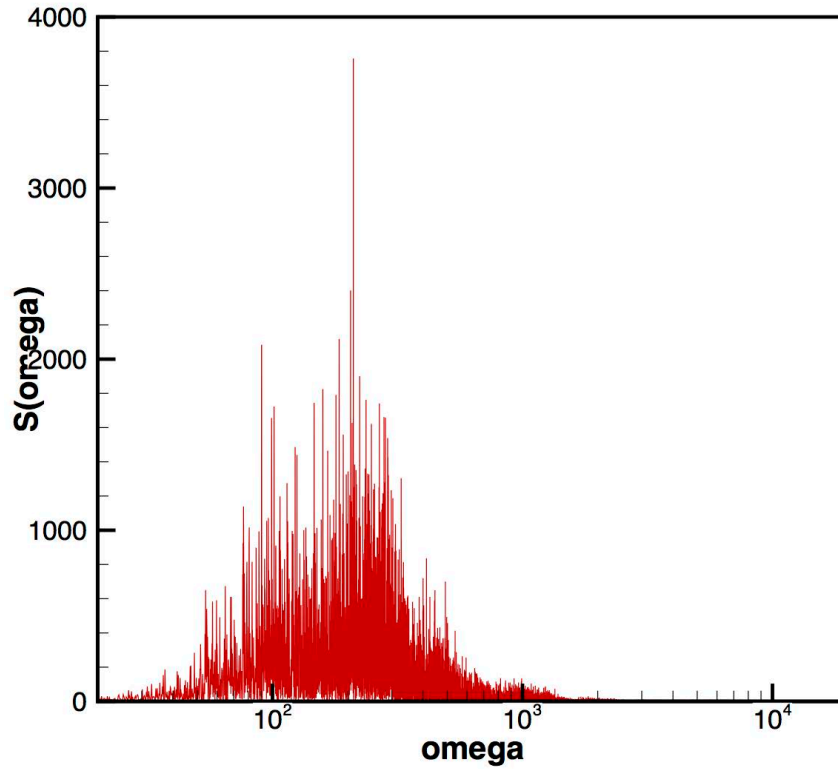
where ω is the angular frequency ($\omega = 2\pi f$, f is the frequency). In the present work, the integral in (1) is evaluated by the Simpson's rule.

In the Two-step Method, one first computes the autocorrelation function $R(\tau)$ using a real time noise sample of length $2T_0$. Then the spectrum, $S(\omega)$, is found by taking the Fourier transform of $R(\tau)$. Thus the first step is to compute,

$$R(\tau) \Big|_{T_0 \rightarrow \infty} = \frac{1}{2T_0} \int_{-T_0}^{T_0} p(t) p(t+\tau) dt \quad (3)$$

And the second step is to compute,

$$S(\omega) \Big|_{T_0 \rightarrow \infty} = \frac{1}{2\pi} \int_{-T_0}^{T_0} R(\tau) e^{i\omega\tau} d\tau \quad (4)$$

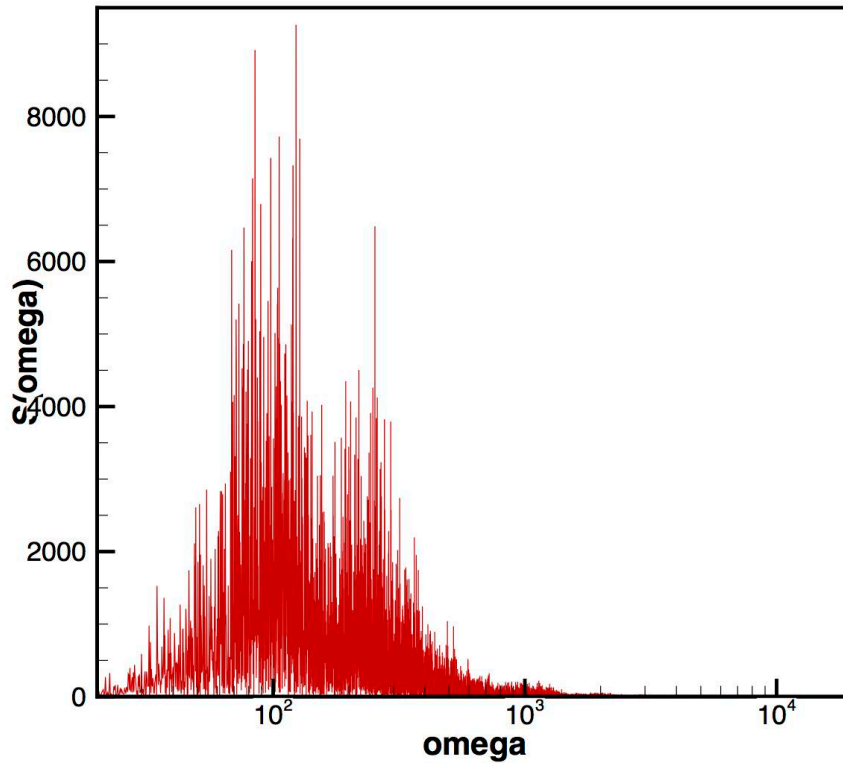


Fourier transform for
MIL power setting, 50 ft. arc, 141° inlet angle

Parameters for auto-correlation program

N	1400000
Δt	0.000005 s
time interval	2 - 8 s
sampling rate	200000 / s

Figure 1. Spectrum computed by the direct method using real time data measured by a microphone located at 141° on a 50 ft arc at Mil power.

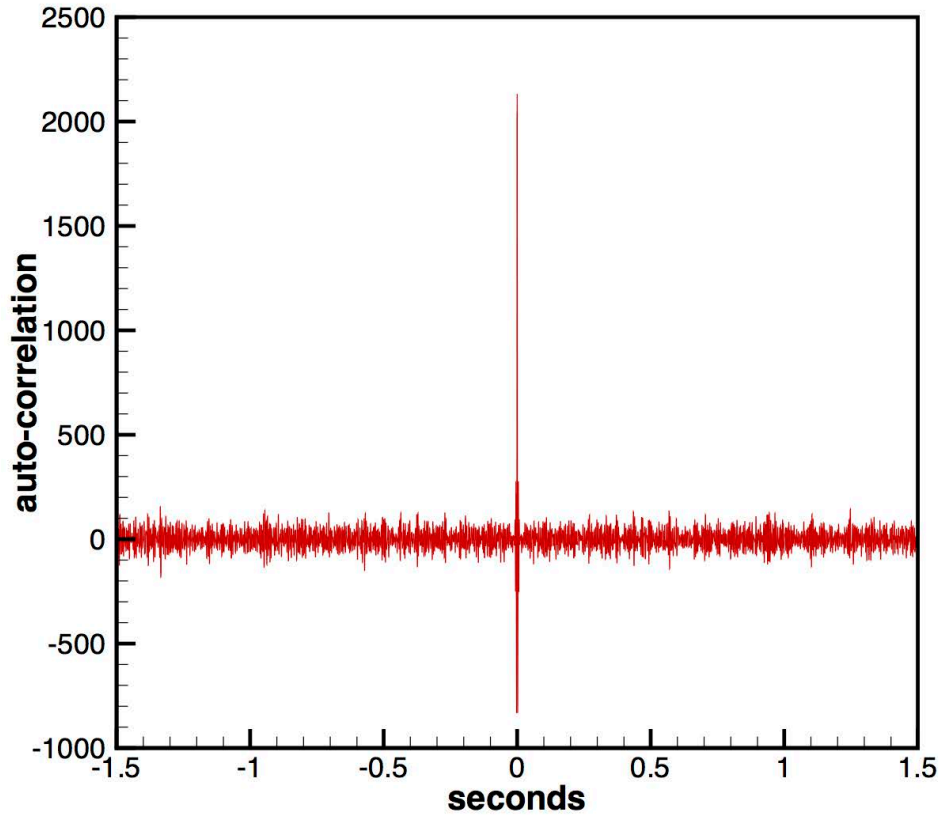


Fourier transform for
MaxAB power setting, 50 ft. arc, 141° inlet angle

Parameters for auto-correlation program
 N 1400000
 Δt 0.000005 s
time interval 2 - 8 s
sampling rate 200000 / s

Figure 2. Spectrum computed by the direct method using real time data measured by a microphone located at 141° on a 50 ft arc at MaxAB power.

Figure 1 shows the computed noise spectrum at 141° inlet angle on a 50 ft arc at Mil power using the direct computation method of equations (1) and (2). Obviously, the computed spectrum is unacceptable. It is overwhelmed by spurious high frequency oscillations. Figure 2 shows a similar result at MaxAB power. It is not clear at this point why this computation method does not yield an acceptable spectrum.



80N2 power setting, 50 ft. arc, 141° inlet angle

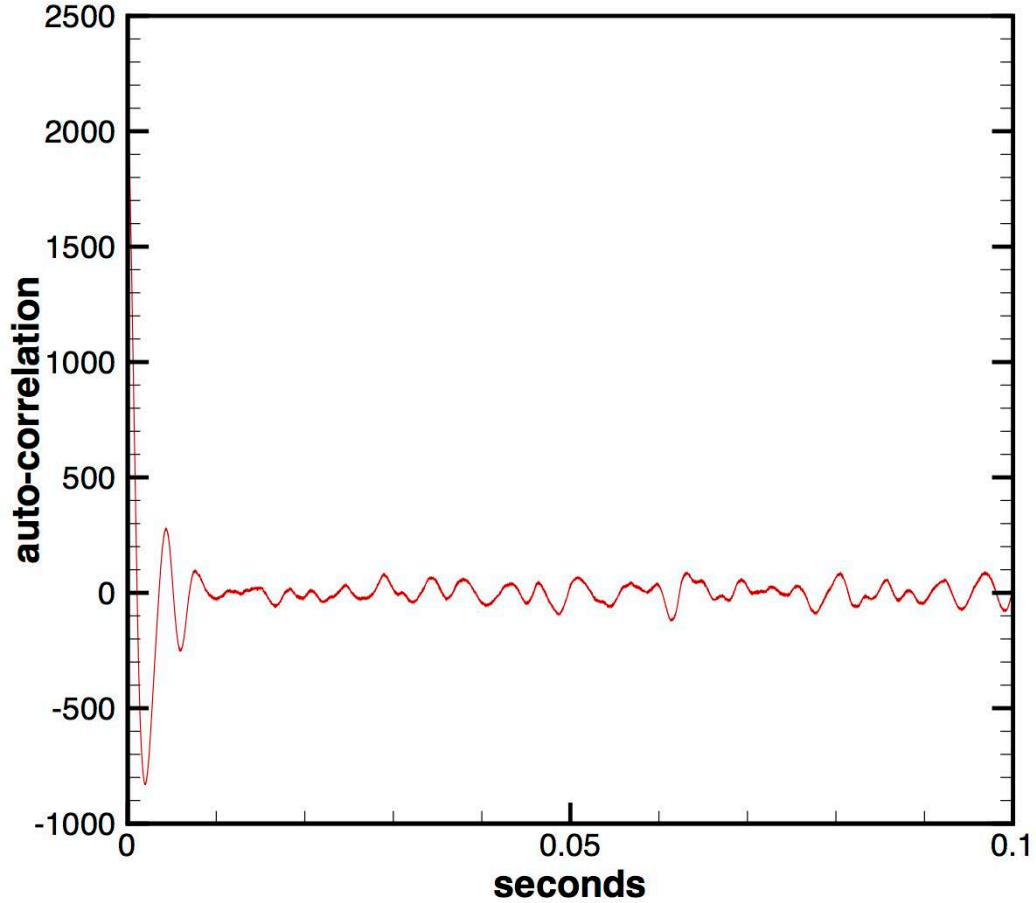
Parameters for auto-correlation program

N	1200001
Δt	0.000005 s
$N_{int\ max}$	3000
N_r	3000
τ_{max}	1.5
$T_{int\ max}$	1.5
time interval	2 - 8 s
sampling rate	200000 / s

Figure 3. Autocorrelation function at 141° inlet angle at 80N2 power.

Naturally, we turned to the use of the Two-step Method at this point. On following this method, we first computed the autocorrelation function $R(\tau)$ using a data sample of 6-second length. Figure 3 shows a plot of the autocorrelation function computed using noise data measured by the same microphone at 80N2 power. This function has two distinct features. There is a very narrow spike for very small τ . In addition, there is still non-zero correlation for $\tau > 1.5$ sec. For a jet with exit velocity at around 1200 ft/sec, 1.5 sec means a jet column of 1800 feet long. Surely, there is no correlation of jet turbulence at such a distance apart. The fact that there is still non-zero correlation at such a large delay time can only mean that there is intrinsic noise (probably most of them are electronic noise) in the data. This is, perhaps, the reason why Direct Computation Method fails to give a meaningful spectrum. In order to have a better idea

of the intrinsic noise, an enlarged plot of figure 3 is provided in figure 4. The intrinsic noise appears to be quasi-periodic with an averaged period of 0.005 sec and an amplitude of 100 pascal². Figure 5 shows an even larger enlarged autocorrelation function with $-0.02 \text{ sec.} \leq \tau \leq 0.02 \text{ sec.}$ The peak has a magnitude of 2100 pascal².

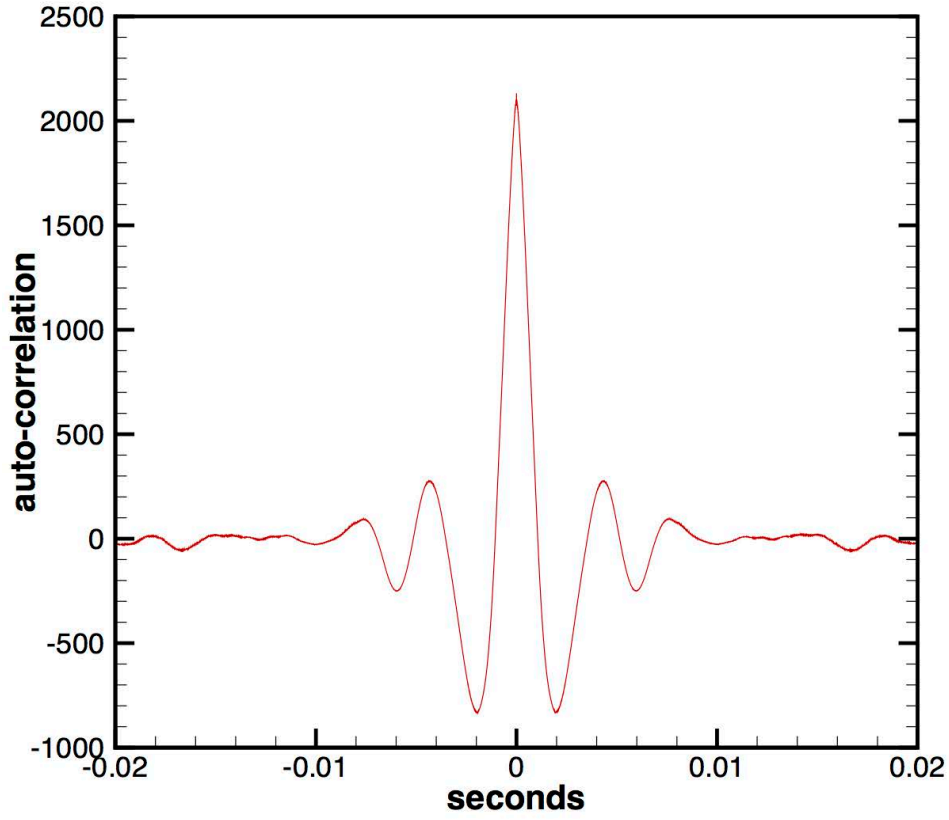


80N2 power setting, 50 ft. arc, 141° inlet angle

Parameters for auto-correlation program

N	1200001
Δt	0.000005 s
$N_{int \ max}$	3000
N_{τ}	3000
τ_{max}	1.5
$T_{int \ max}$	1.5
time interval	2 - 8 s
sampling rate	200000 / s

Figure 4. An enlarged autocorrelation function of figure 3.



80N2 power setting, 50 ft. arc, 141° inlet angle

Parameters for auto-correlation program

N	1200001
Δt	0.000005 s
$N_{int\ max}$	3000
N_r	3000
τ_{max}	1.5
$T_{int\ max}$	1.5
time interval	2 - 8 s
sampling rate	200000 / s

Figure 5. A much enlarged autocorrelation function in the interval of -0.02 s to 0.02 s .

Now, to be able to compute a meaningful noise spectrum, it is clear that the intrinsic noise has to be removed first. It is noted that the noise to signal intensity ratio is around $2100/100 \approx 21$. So the removal of the unwanted noise from the autocorrelation function should have a relatively minor effect on the function. This line of reasoning suggests that we may, as a first approximation, insert a boxcar window function in the integral of equation (4). That is, equation (4) is to be replaced by,

$$S(\omega) = \frac{1}{2\pi} \int_{-T_0}^{T_0} R(\tau) B(\tau; \tau_0) e^{i\omega\tau} d\tau = \frac{1}{2\pi} \int_{-\tau_0}^{\tau_0} R(\tau) e^{i\omega\tau} d\tau \quad (6)$$

where the boxcar window function $B(\tau:\tau_0)$ is given by,

$$B(\tau:\tau_0) = \begin{cases} 0, & |\tau| > \tau_0 \\ 1, & |\tau| \leq \tau_0 \end{cases} \quad (7)$$

Another way to state the effect of the window function is that the autocorrelation function is clipped at $\tau = -\tau_0$ and $\tau = \tau_0$. This leaves the autocorrelation function non-zero only in the interval of $-\tau_0 \leq \tau \leq \tau_0$. τ_0 is the parameter that controls the size of the boxcar window function or the clipping window.

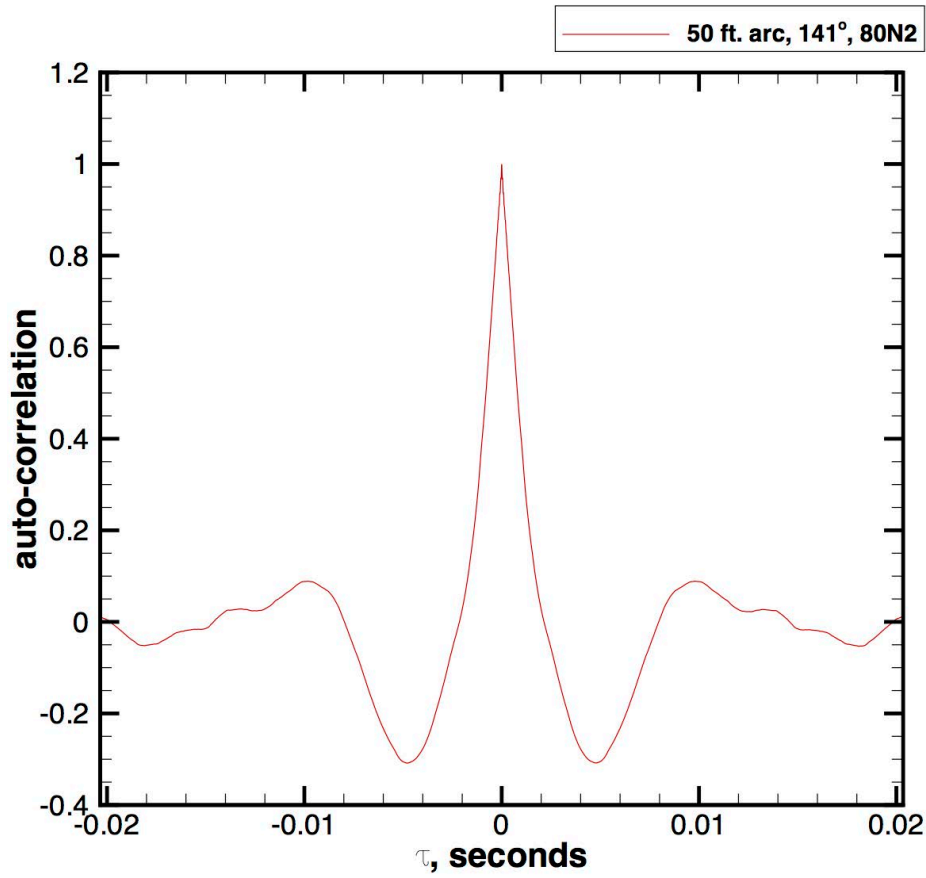


Figure 6. Autocorrelation function at 141° at 80N2 power clipped at $\tau_0 = 0.02$ sec.

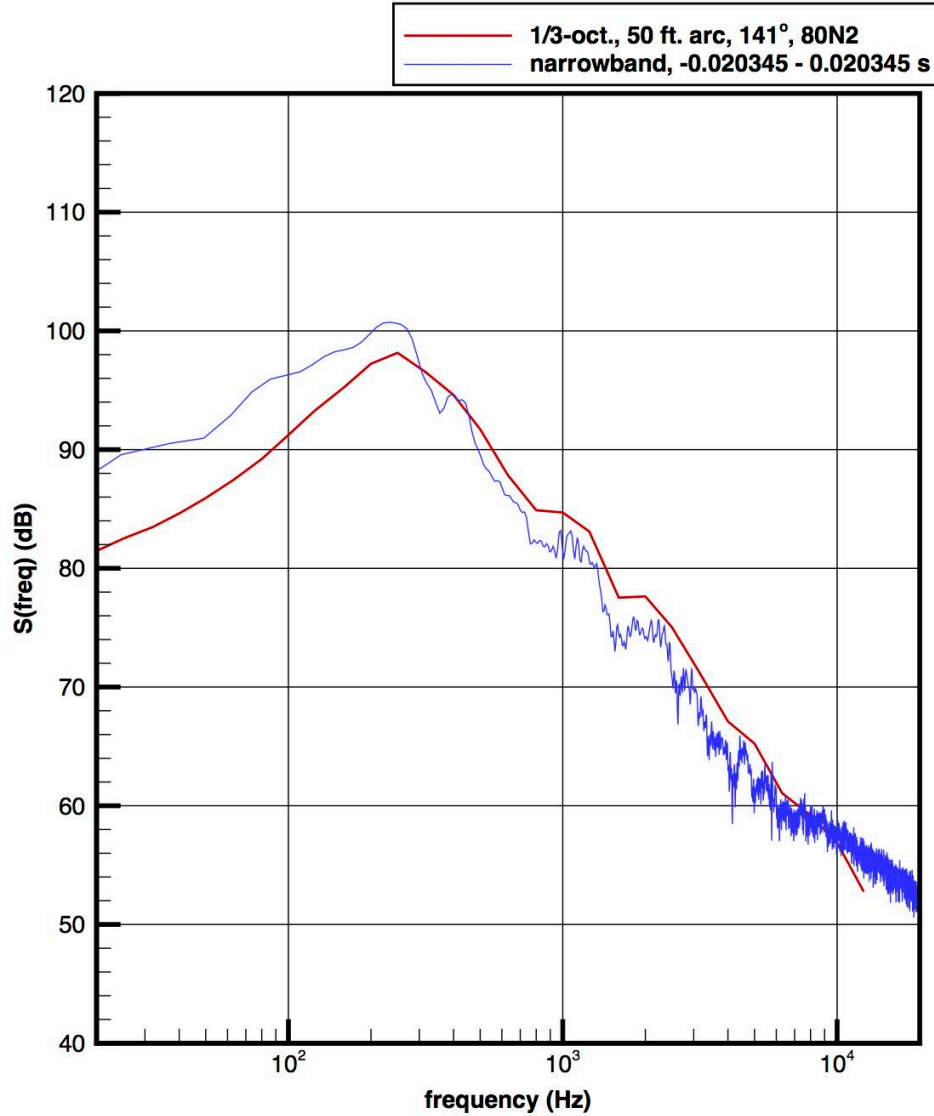


Figure 7. Narrow band spectrum (blue) corresponding to the autocorrelation function of figure 6. Red curve is the 1/3 octave band spectrum.

2. Effect of the size of the window function

It is natural to expect the size of the window function to have an impact on the computed narrow band spectrum. To demonstrate the effect on the choice of τ_0 , three values of τ_0 are chosen and the corresponding spectrum $S(\omega)$ are computed according to equation (6). The three values of τ_0 are 0.02, 0.009065 and 0.005145 sec. Figure 6 shows the normalized autocorrelation function clipped at $\tau_0 = 0.02$ sec. Figure 7 shows the corresponding narrow band spectrum. The relatively smooth curve in red is the

spectrum from the 1/3 octave band data. It is readily seen that there is reasonably good agreement between the two spectra except at low frequencies (frequencies less than 200 Hz). It will be shown later that the low frequency difference is not important from an energy consideration.

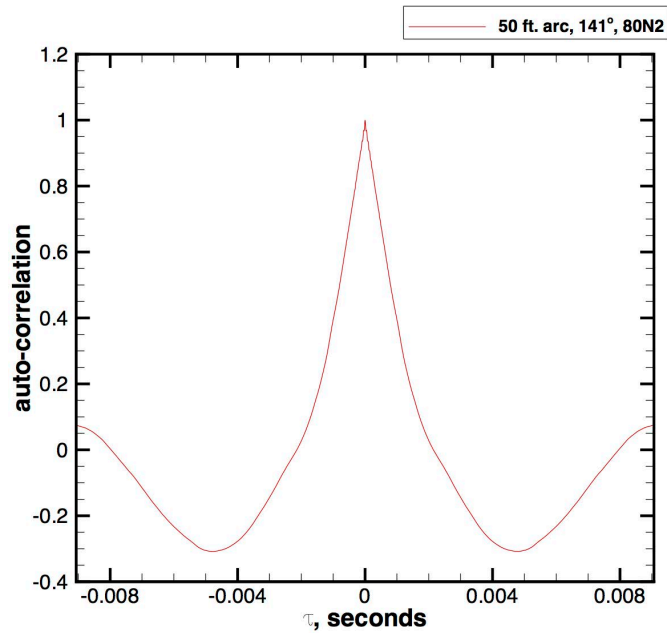


Figure 8. Autocorrelation function at 141^0 at 80N2 power clipped at $\tau_0 = 0.009065$ sec.

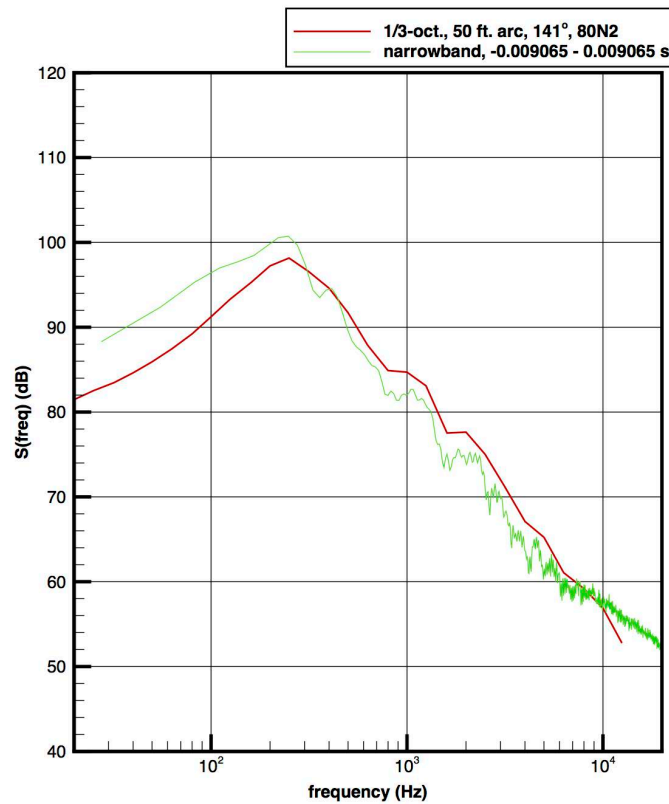


Figure 9. Narrow band spectrum (green) corresponding to the autocorrelation function of figure 8. Red curve is the 1/3 octave band spectrum.

Figure 8 shows the normalized autocorrelation function clipped at $\tau_0 = 0.009065$ sec. Figure 9 is the corresponding narrow band spectrum. On comparing the two spectra in figures 7 and 9, it is seen that the use of a smaller clipping window reduces some of the high frequency oscillations.

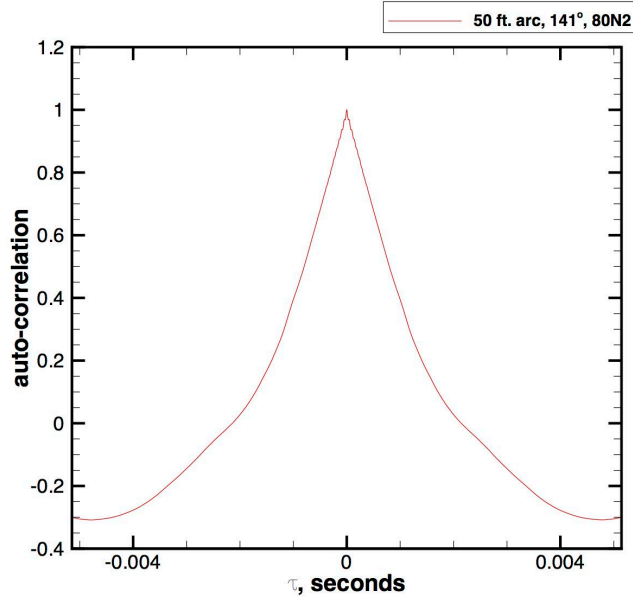


Figure 10. Autocorrelation function at 141° at 80N2 power clipped at $\tau_0 = 0.005145$ sec.

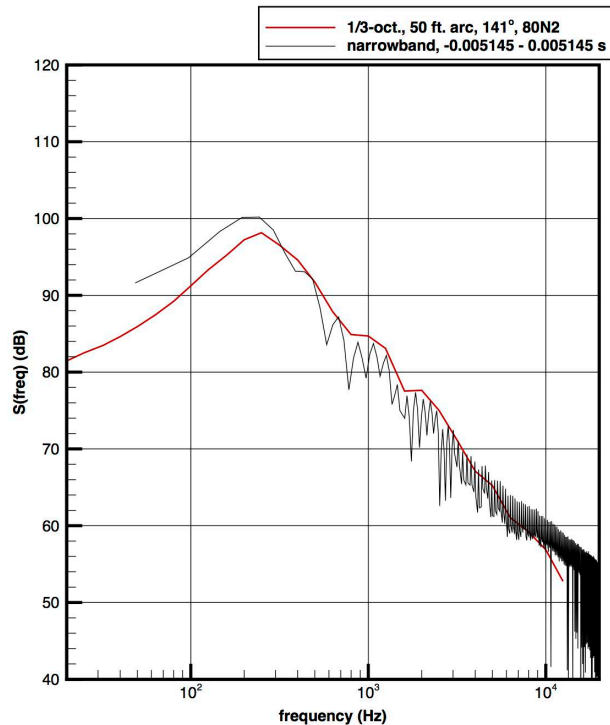


Figure 11. Narrow band spectrum (black) corresponding to the autocorrelation function of figure 10. Red curve is the 1/3 octave band spectrum.

Figure 10 is the normalized autocorrelation function clipped at $\tau_0 = 0.005145$ sec. The boxcar window function is very small in this case. Also there is a large jump in the value of the autocorrelation function at the clipping points. Figure 11 shows the computed narrow band spectrum for this case. The spectrum has numerous oscillations and is, therefore, not acceptable even though the overall shape matches well with the 1/3 octave spectrum and the spectra in figures 7 and 9.

We have carried out further experimentation on the choice of the size of the window function. Our finding is that, generally speaking, for the F-18E data set, it is better to set τ_0 to be less than 0.02 sec. In addition, it is best to chose a value of τ_0 at which the autocorrelation is zero or nearly zero. The reason for this recommendation is that this choice will avoid having a not too small discontinuity in the autocorrelation function. In this way, the Gibbs phenomenon in Fourier series would be avoided. We suspect that the oscillations in the spectrum in figure 11 are the artifacts of the Gibbs phenomenon.

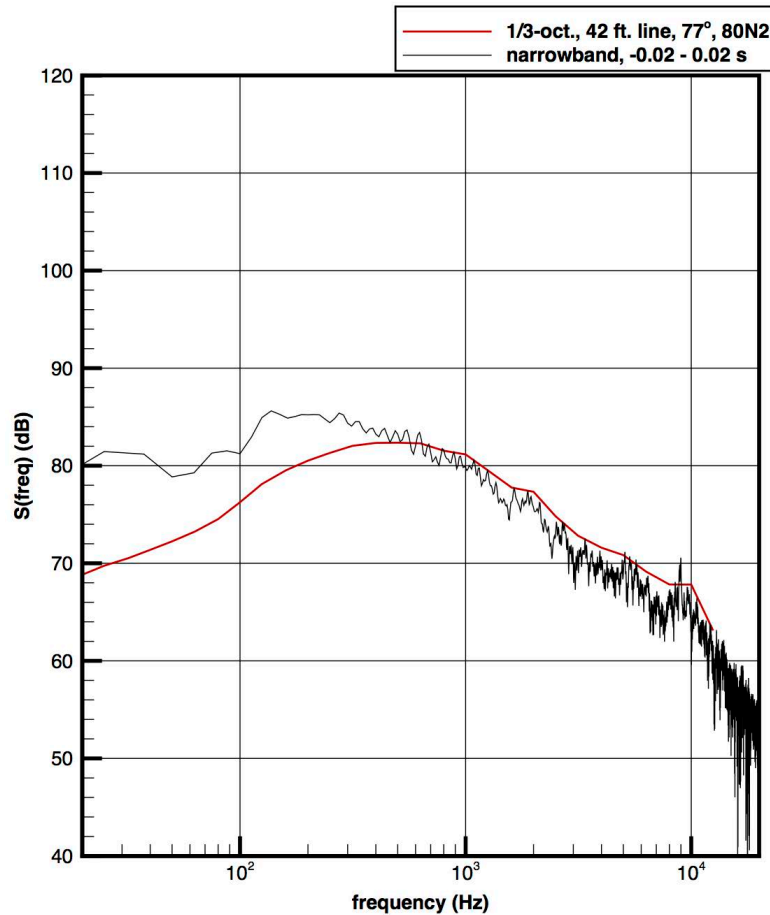


Figure 12. Narrow band spectrum at 77° and at 80N2 power level computed with clipping window $\tau_0 = 0.02$ sec.

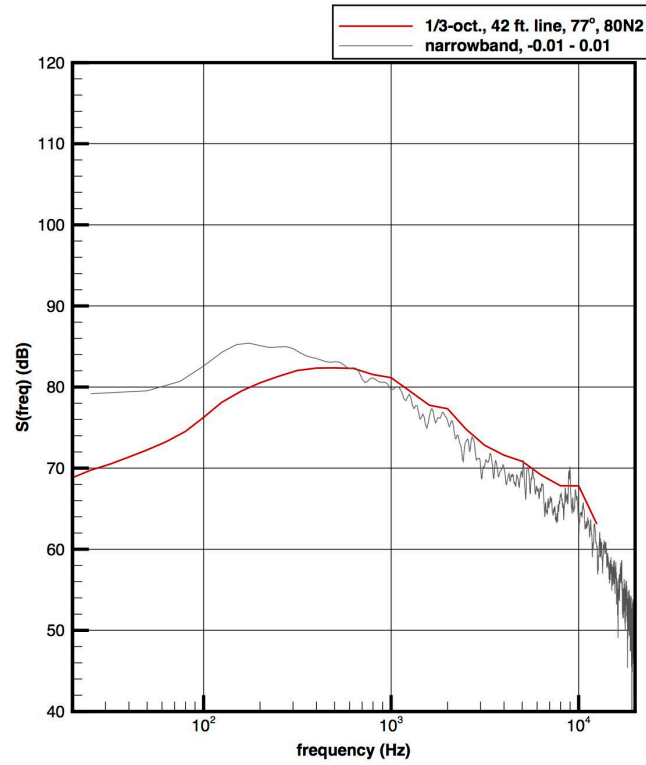


Figure 13. Narrow band spectrum at 77^0 and at 80N2 power level computed with clipping window $\tau_0 = 0.01$ sec.

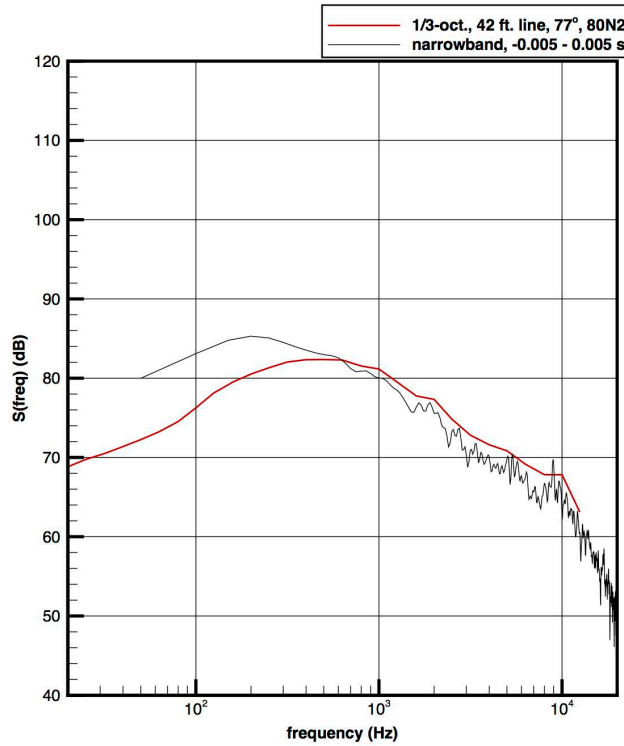


Figure 14. Narrow band spectrum at 77^0 and at 80N2 power level computed with clipping window $\tau_0 = 0.005$ sec.

As another example to illustrate the effect of the size of clipping window on the computed spectrum, we consider the case of the microphone data measured at 77° on the 42 ft line at 80N2 power level. Figure 12 is the spectrum computed with a clipping window of $\tau_0 = 0.02$. This is the largest clipping window we recommend to use. Figure 13 is the spectrum computed with $\tau_0 = 0.01$. This spectrum is essentially the same as that in figure 12. However, the spectrum in figure 13 has less high frequency oscillations in the high frequency part of the spectrum. Figure 14 is the spectrum with an even smaller clipping window. The value of τ_0 is 0.005. The spectrum is practically free of high frequency oscillations. We believe this is nearly the optimum size clipping window for this microphone data.

3. Comparisons between narrow band spectra and 1/3 octave band spectra

With the understanding of how to best compute narrow band spectra, we will now present comparisons between narrow band spectra (1 Hz band width) and 1/3 octave band spectra (converted to 1 Hz band width). The purpose of making the comparisons is to assure that, by and large, there is consistency between these two types of data. Below, we will first present spectra measured at 80N2 power level to be followed by the spectra measured at Mil power and then at MaxAB power.

A. Spectra at 80N2 power

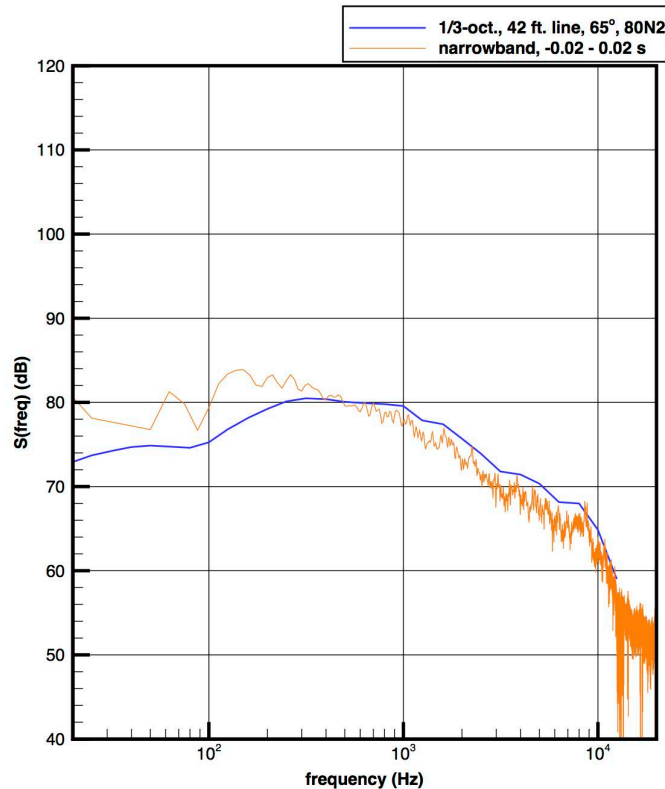


Figure 15. Comparison of narrow band and 1/3 octave band spectra. 65° at 80N2 power.

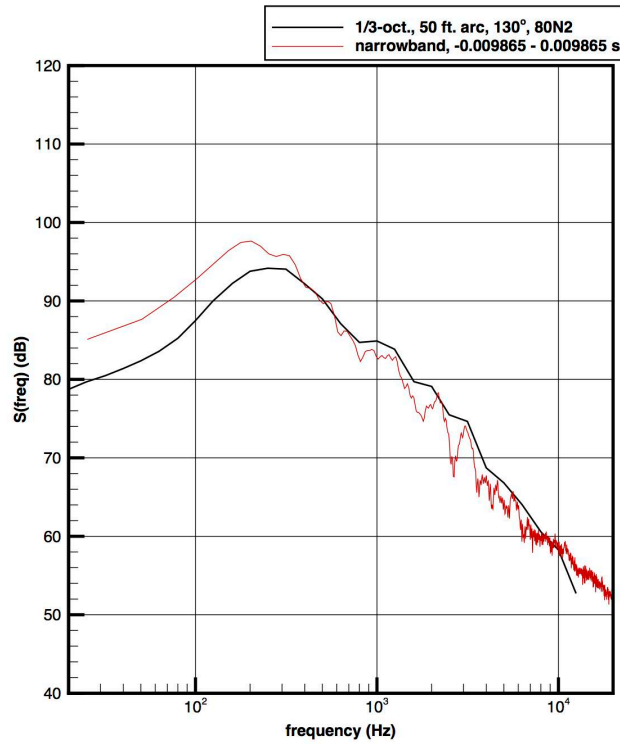


Figure 16. Comparison of narrow band and 1/3 octave band spectra. 130° at 80N2 power.

B. Spectra at Mil power

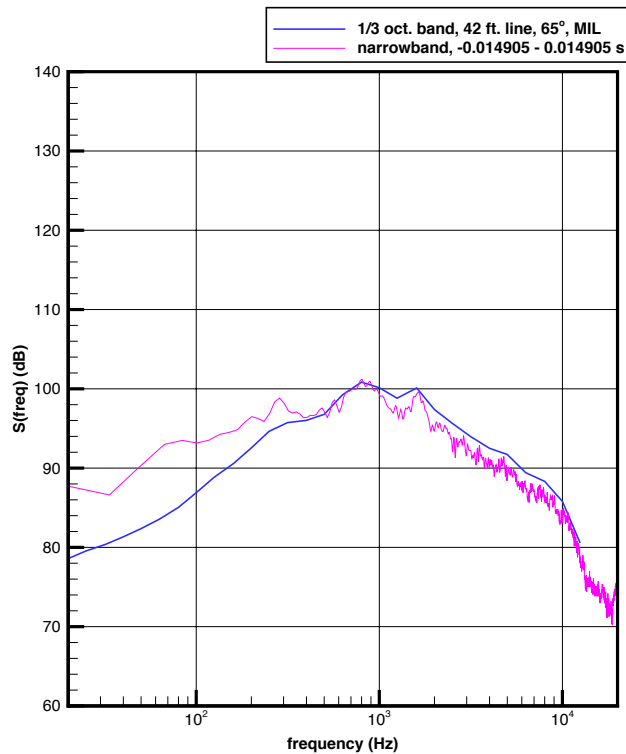


Figure 17. Comparison of narrow band and 1/3 octave band spectra. 65° at Mil power.

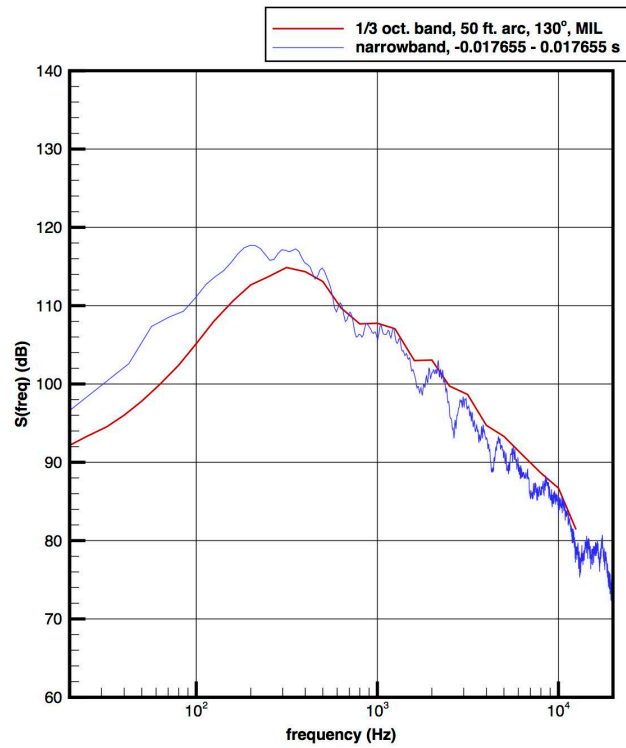


Figure 18. Comparison of narrow band and 1/3 octave band spectra. 130° at Mil power.

C. Spectra at MaxAB power

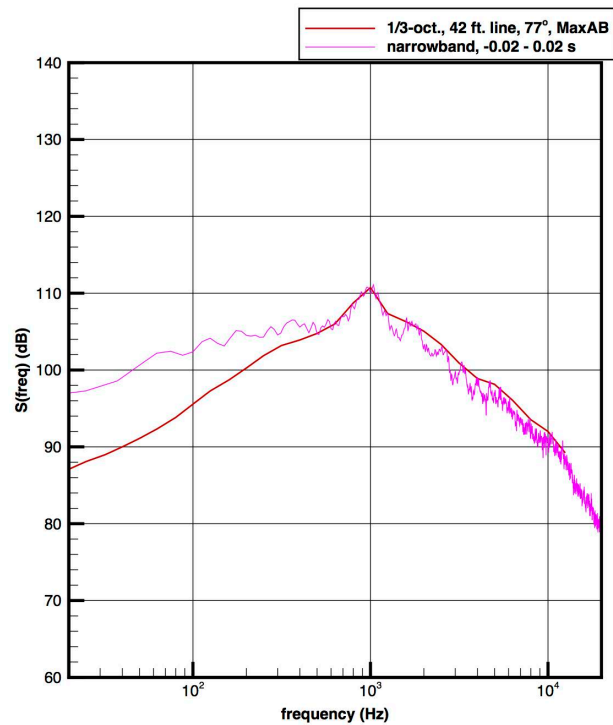


Figure 19. Comparison of narrow band and 1/3 octave band spectra. 77° at MaxAB power.

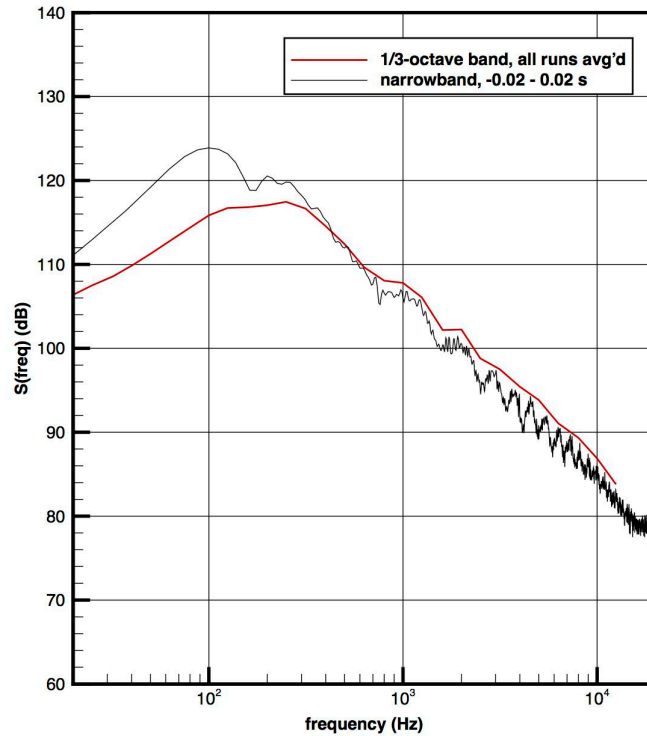


Figure 20. Comparison of narrow band and 1/3 octave band spectra. 141^0 at MaxAB power.

4. Spectra with frequency plotted in a linear scale

All the spectra displayed above are plotted in a log scale in frequency. The reason to plot frequency in a log scale is that in log scale 3 decades of frequency data can be easily exhibited in a single figure. On the other hand, noise spectrum is an energy plot. The area under the curve is the total acoustic energy radiated in a specific direction. The use of log scale will, inevitably, distort the bandwidth and hence the relative energy in each band. Another unintended consequence of using log scale for frequency is that the high portion of the spectrum might not be sufficiently well resolved for a reader to observe. For the above reasons, we believe it is useful to display some of the noise spectra in a linear scale in frequency. These spectra are exhibited below grouped together by engine power level.

a. 80N2 power

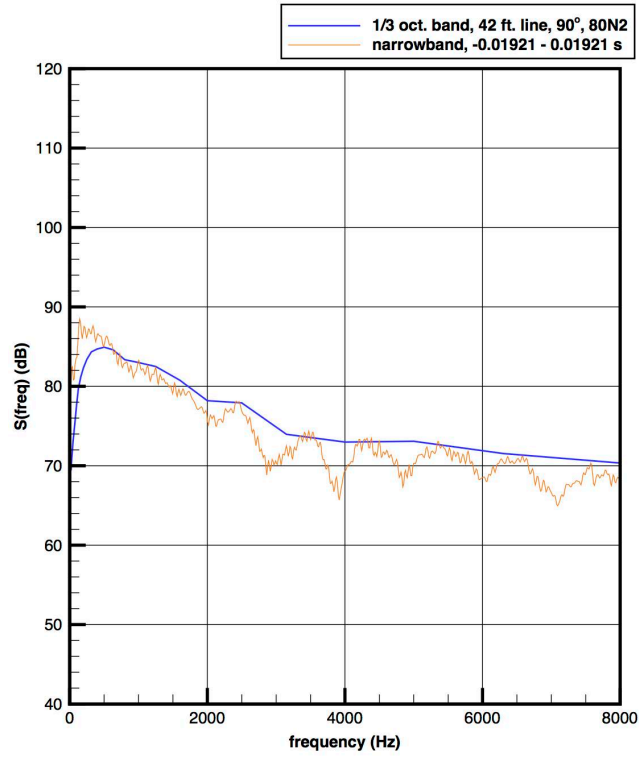


Figure 21. Noise spectrum at 90^0 with frequency in linear scale. Blue curve is the spectrum from 1/3 octave band data.

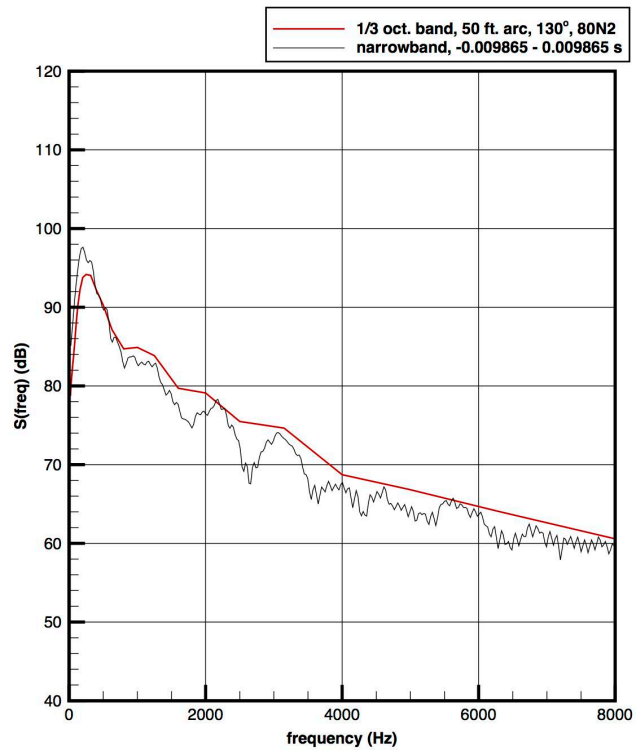


Figure 22. Noise spectrum at 130^0 with frequency in linear scale. Red curve is the spectrum from 1/3 octave band data.

b. Mil power

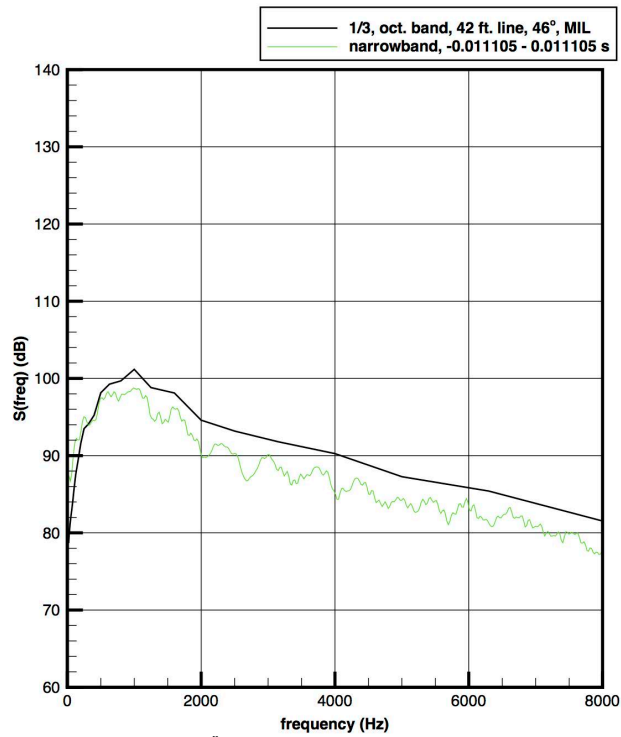


Figure 23. Noise spectrum at 46^0 with frequency in linear scale. Black curve is the spectrum from 1/3 octave band data.

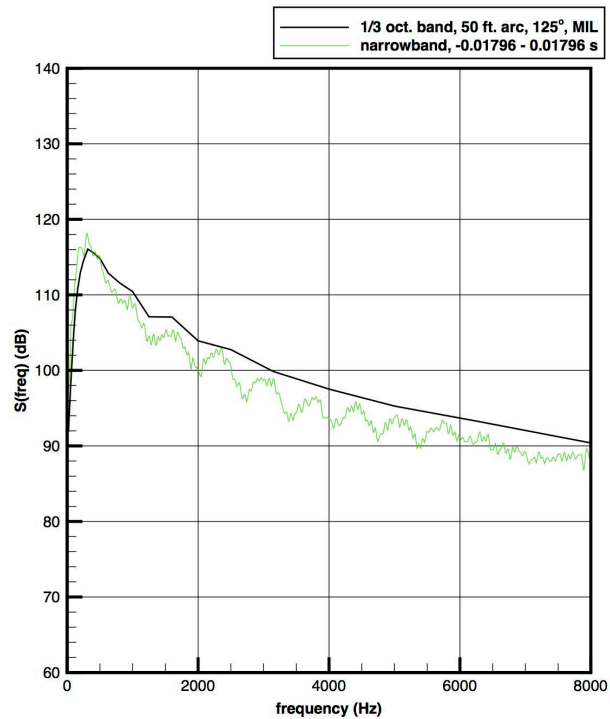


Figure 24. Noise spectrum at 125^0 with frequency in linear scale. Black curve is the spectrum from 1/3 octave band data.

c. MaxAB power

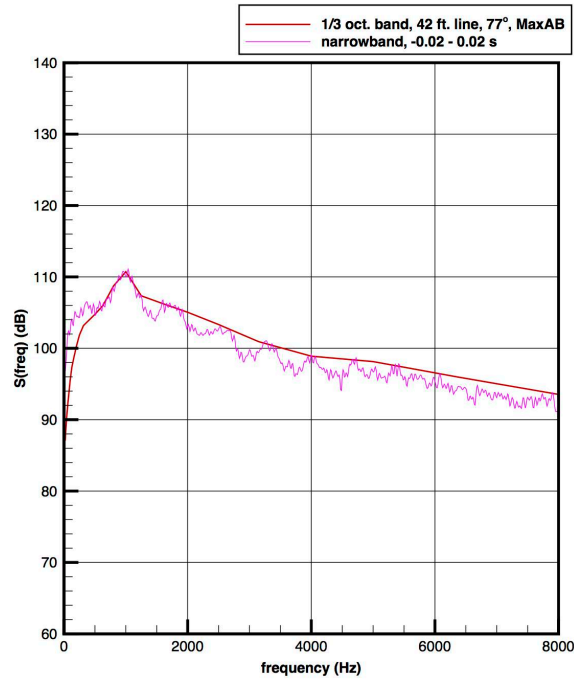


Figure 25. Noise spectrum at 77^0 with frequency in linear scale. Red curve is the spectrum from 1/3 octave band data.

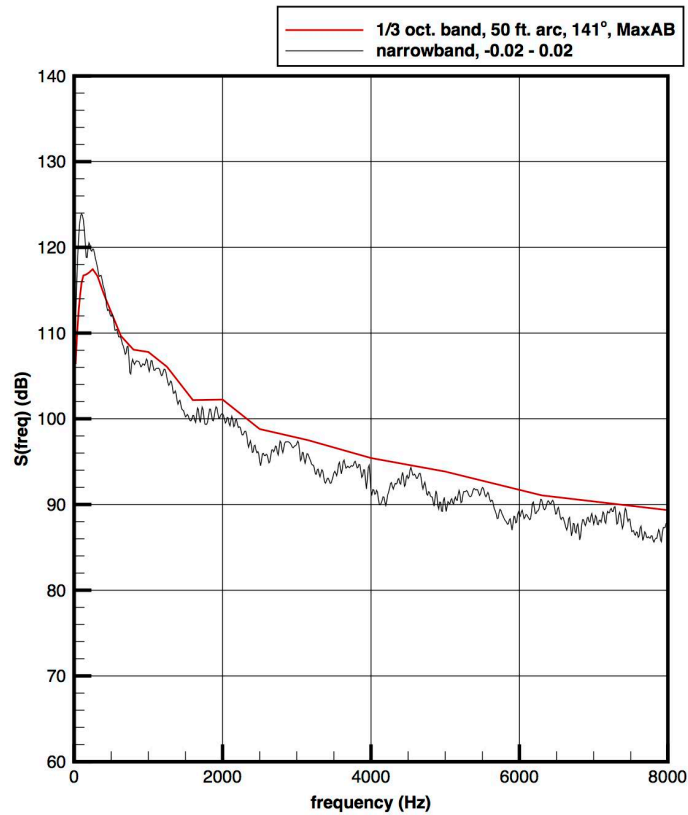
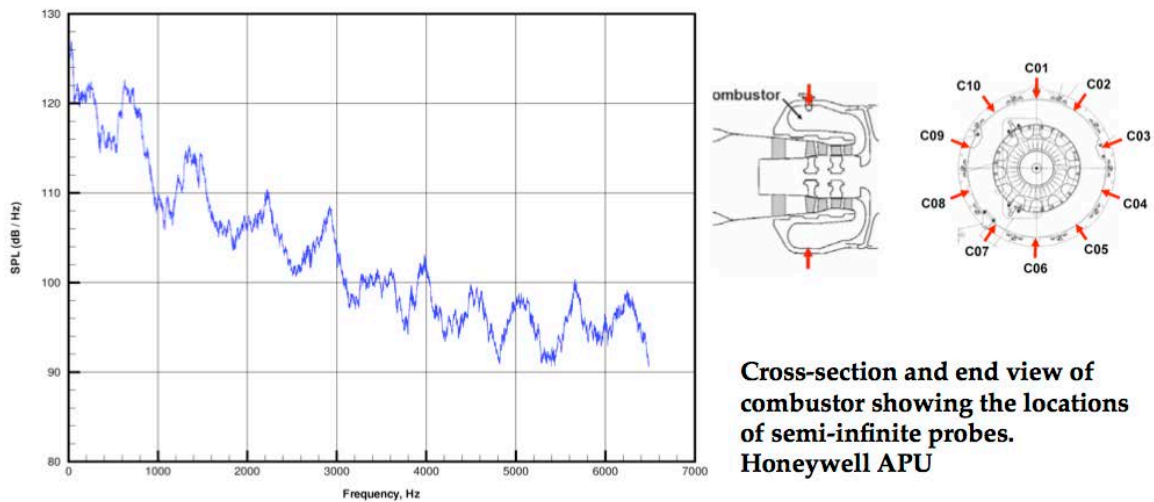


Figure 26. Noise spectrum at 141^0 with frequency in linear scale. Red curve is the spectrum from 1/3 octave band data.



Pressure spectrum measured at C01

Figure 27. Combustor resonance tones measured inside a Honeywell APU by Schuster and Mendoza.

It is important to observe that regardless of the power level of the engine and the direction of radiation all noise spectra (figures 21 to 26) contain distinct peaks. It is not a single peak but a series of quasi-periodic peaks. Naturally, these are tones from the engine. The question one would ask is ‘what are these tones?’. Experience with tones from commercial jet engines suggests that they may be tones generated by the fan. However, fan tones are usually sharp (well spaced apart) and have narrow half-widths. The peaks in the above spectra do not seem to possess these characteristics. The peaks appear to overlap with the neighboring peaks. The half-widths are not small. It is also known that combustors in jet engines do generate strong tones that may or may not radiate outside the engine. For example, figure 27 is a noise spectrum containing a series of combustor resonance tones. The spectrum was measured by Schuster and Mendoza (X3-NOISE/CEAS Combustion Noise Workshop, 27-28 Sept. 2007, Lisbon, Portugal) inside a Honeywell APU. The row of tones in Figure 27 closely resembles those in figures 21 to 26. This leads to the possibility that F-18E aircraft tones are combustor resonances. At this time, in the absence of other independent data, we are unable to conclude whether the tones of F-18E aircraft are fan tones or combustor resonances.

It is also worthwhile to remark that when the spectrum is plotted in a linear scale in frequency, the low frequency differences between the spectra from narrow band data and those from 1/3 octave band data do not seem to be significant. There is little difference in the acoustic energy (area under the curve) between the two types of data.

Future research

We anticipate that our next quarterly progress report will concentrate on our numerical simulation of indirect combustion noise generation in military styled nozzles.

REPORT DOCUMENTATION PAGE					Form Approved OMB No. 0704-0188	
<p>The public reporting burden for this collection of information is estimated to average 1 hour per response, including the time for reviewing instructions, searching existing data sources, gathering and maintaining the data needed, and completing and reviewing the collection of information. Send comments regarding this burden estimate or any other aspect of this collection of information, including suggestions for reducing the burden, to Department of Defense, Washington Headquarters Services, Directorate for Information Operations and Reports (0704-0188), 1215 Jefferson Davis Highway, Suite 1204, Arlington, VA 22202-4302. Respondents should be aware that notwithstanding any other provision of law, no person shall be subject to any penalty for failing to comply with a collection of information if it does not display a currently valid OMB control number.</p> <p>PLEASE DO NOT RETURN YOUR FORM TO THE ABOVE ADDRESS.</p>						
1. REPORT DATE (DD-MM-YYYY)		2. REPORT TYPE			3. DATES COVERED (From - To)	
4. TITLE AND SUBTITLE				5a. CONTRACT NUMBER		
				5b. GRANT NUMBER		
				5c. PROGRAM ELEMENT NUMBER		
6. AUTHOR(S)				5d. PROJECT NUMBER		
				5e. TASK NUMBER		
				5f. WORK UNIT NUMBER		
7. PERFORMING ORGANIZATION NAME(S) AND ADDRESS(ES)					8. PERFORMING ORGANIZATION REPORT NUMBER	
9. SPONSORING/MONITORING AGENCY NAME(S) AND ADDRESS(ES)					10. SPONSOR/MONITOR'S ACRONYM(S)	
					11. SPONSOR/MONITOR'S REPORT NUMBER(S)	
12. DISTRIBUTION/AVAILABILITY STATEMENT						
13. SUPPLEMENTARY NOTES						
14. ABSTRACT						
15. SUBJECT TERMS						
16. SECURITY CLASSIFICATION OF:			17. LIMITATION OF ABSTRACT	18. NUMBER OF PAGES	19a. NAME OF RESPONSIBLE PERSON	
a. REPORT	b. ABSTRACT	c. THIS PAGE			19b. TELEPHONE NUMBER (Include area code)	